ELSEVIER

Ecological Modelling 140 (2001) 141–162

ECOLOGICAL MODELLING

www.elsevier.com/locate/ecolmodel

A dynamic modeling approach to simulating socioeconomic effects on landscape changes

Yeqiao Wang *, Xinsheng Zhang

Department of Natural Resources Science, University of Rhode Island, Kingston, RI 02881, USA

Abstract

Modeling and simulating the effects of human factors on landscape change remain as challenges for ecological studies. In this paper, we present a dynamic landscape simulation (DLS) approach to elucidate human-induced landscape changes for a 5104 km^2 study area within the Chicago metropolitan region. The DLS consists of an urban growth simulation submodel and a land-cover simulation submodel. This approach simulates urban land-use expansion by incorporating socioeconomic and demographic data and predicts changes in the landscape as a result of urban expansion. A utility function of spatial choice and a methodology for the construction of that utility function were developed to execute the process. The approach, with dynamic adjustment of transition structures (i.e. the transition potentials, threshold and rate), overcomes the shortcomings of static and statistical models that use a constant transition probability in simulation modeling. It also allows selected economic principles to be integrated into landscape simulation. In this study, historical land-cover and census data were applied to derive transition thresholds and transition rates of the land cover changes. Comparison of the 1997 land-cover maps derived by a DLS simulation and by the classification of Landsat Thematic Mapper (TM) remotely sensed data indicated that a 62.3% overall agreement was achieved among the changed areas. Landscape simulations of the study area from 1997 to 2020 at 5 year time interval were prepared. The results depicted the trends of landscape change in this large urban setting area.

Keywords: Dynamic model; Utility function; Urban growth; Landscape; Simulation; Chicago region

1. Introduction

Landscape pattern has four basic elements: number, size, shape, and juxtaposition of patches. These elements are important contributors to the interpretation of ecological processes (Gardner et al., 1987; O'Neill et al., 1988; Dunn et al., 1990). Landscapes represent complex ecological systems that operate over broad spatio-temporal scales (O'Neill et al., 1989). Considerable interest has focused on the simulation of landscape dynamics (e.g. Turner, 1987; Turner, et al., 1989; Muller and Middleton, 1994; Boerner et al., 1996; Childress, 1997). Since a landscape pattern at any given time is a stage on which dynamic processes occur, quantitative landscape studies require that time, or temporal change, be considered (Dunn et al., 1990).

* Corresponding author. Tel.: +1-401-8744345; fax: +1-401-8744561.

E-mail address: yqwang@uri.edu (Y. Wang).

0304-3800/01/$ - see front matter
PII: S0304-3800(01)00262-9

Both natural and socioeconomic processes drive landscape change. Among human factors, urban land expansion is one of the main driving forces that changes landscapes and threatens natural ecosystems. Human demand for land and extensive land conversion for economic activities accelerate losses of biodiversity (Ehrlich, 1988; Liu and Ashton, 1998). Socioeconomic and demographic data have, until recently, rarely been linked with other biophysical data in landscape studies (Lo and Faber, 1997). Simulation of human-influenced landscape change remains as a research challenge (Flamm and Turner, 1994).

Modeling approaches that incorporate human factors into landscape simulation have long been explored (Turner, 1987; Hall et al., 1988). Flamm and Turner (1994) tested stochastic simulation models to integrate socioeconomic and ecological information into a spatially explicit transition model of landscape change. Their simulations were designed to compare pixel-based (100 m), patch-based, and ownership-based transition models in order to evaluate the effects of incorporating differing amounts of information about the landscape into the model. Socioeconomic data were applied to construct transition probabilities and introduce human influences into landscape simulations.

When human activities are considered, Markov models which handle stationary processes may not be appropriate, because transition probabilities among landscape states are not constant (Boerner et al., 1996). Traditional cellular automaton (CA) models do not consider variation of transition structures throughout a large study area in which unbalanced human influences on landscapes may occur. A hybrid Markov-cellular automaton (M-CA) model is a new approach in spatio-temporal dynamic modeling (Silvertown et al., 1992; Li and Reynolds, 1997). In M-CA modeling, the Markov process controls temporal dynamics among the cover types through the use of transition probabilities (e.g. Turner, 1987; Silvertown et al., 1992). Spatial dynamics are controlled by local rules determined either by the cellular automaton mechanism (neighborhood configuration) or by its association with the transition probability (e.g. Silvertown et al., 1992). It has been recognized that GIS data have great potential for M-CA modeling, both in the model development and simulation phases (Zhou and Liebhold, 1995). A major advantage of the M-CA approach is that GIS and remote sensing data can be efficiently incorporated (Li and Reynolds, 1997). In particular, temporal GIS data can be used to define initial conditions, to parameterize M-CA models, to calculate transition probabilities and to determine the neighborhood rules. Although the potential has been discussed by Li and Reynolds (1997), multitemporal remote sensing data and the derivatives of sequentially developed GIS data have rarely been directly incorporated into dynamic simulation modeling.

Since urban land expansion is one of the main factors that affects natural ecosystems, a dynamic mechanism in urban growth simulation is a key for revealing human impacts on landscape change. GIS spatial analysis provides support for formulating operational and practical urban and regional models. In general, four categories of GIS-based models have been applied to predict the evolution of urban and regional spatial structures. These include statistical models (Jensen et al., 1994); Lowry-type models (Parrot and Stutz, 1991); spatial choice behavior models (Zhang and He, 1997); and CA models (Xie, 1996; Clarke and Gaydos, 1998; Wu, 1998). Spatio-temporal interactions among the spatial compartments and subsystems were not considered as an integral component of the models. Most of these models cannot describe dynamic structures of urban systems when spatial interactions among system elements are required and when the dynamic evolution of urban spatial structure needs to be considered.

In order to reveal human-induced landscape change, we developed a dynamic landscape simulation (DLS) approach. The DLS incorporates and quantifies socioeconomic and demographic factors using utility functions of spatial choice. This new approach differs from the previous static and statistical models in that it enables economic principles, such as utility and marginal utility, to be imbedded directly in landscape simulation. Dynamic adjustments of transition rates and thresholds were implemented in the DLS coupled

by the use of multiscale spatial units. The DLS creates a new mechanism to study the impact of human factors on landscape dynamics. Therefore, the objective of this paper is to illustrate the DLS modeling approach and the testing results. We first introduce the model structure. Then, we discuss the methods for model construction. Finally, as an application example, we simulate the landscape change within the metropolitan Chicago area using the DLS approach.

2. Methods

2.1. Study area

The study area is located in a semicircular zone between 30 and 65 km from the center of downtown Chicago and is about 5104 km^2 in area. The Chicago metropolitan area contains some of the world's best remaining patches of endangered natural communities. This significant concentration of rare natural ecosystems includes eastern tallgrass prairie, oak-savanna, open woodland, and wooded and prairie wetland. The existing patches are small and isolated. Long-term survival of these communities depends on proper management of much larger, restorable acreage that surrounds and connects the high-quality remnants. Like most metropolitan areas, the Chicago region has experienced dramatic land-cover change in the past three decades. Population increase and employment-related decentralization of population are among the dominant driving factors that result in landscape change. For example, from 1970 to 1990, the region's population and employment increased by 4 and 21%, respectively, while the urban land area increased by 47%. Land-cover changes occurred mostly in the suburban areas where there are concentrations of natural preserves. As recently projected by the U.S. Bureau of the Census and endorsed by the Northeastern Illinois Planning Commission (NIPC), the Chicago region's population and employment will grow by the year 2020 to more than 9 million and to 5.3 million, a 25 and 37% increase from 1990, respectively (NIPC, 1998). The impacts of the projected population and employment increases on the region's landscape are unknown. Urban land expansion accelerates fragmentation and degradation of natural communities in this large urban setting environment. What the effects of socioeconomic and demographic changes on the landscape will be remains a question to answer.

Distance from downtown Chicago is considered an important character of the regional landscape. A half-ring pattern can be observed from both Landsat images and the derivatives of land cover maps. We subjectively created five concentric zones to quantify the half-ring pattern of the landscape (Fig. 1). The zones divided the Chicago metropolitan region into 0–15 km (Zone I), 15–30 km (Zone II), 30–45 km (Zone III), 45–65 km (Zone IV), and >65 km (Zone V) areas. The distance was measured from the center of Chicago. Land-cover information derived from 1997 Landsat Thematic Mapper (TM) data revealed that Zone III and Zone IV are among the most fragmented areas in the region (Table 1). The highest patch densities of natural areas were observed in Zone III (4.05 patches/km^2) and in Zone IV (3.90 patches/km^2). These two zones were the most changed areas between 1985 and 1997 in urban land expansion (Table 2). Population and employment forecasting data (NIPC, 1998) indicate that the municipalities within or close to these two zones will be among the most changed areas from year 1990–2020. Landscapes within these areas will be affected dramatically by expanding urbanization. Therefore these two zones were selected as the study area.

2.2. Model structure

The DLS consists of an urban growth simulation submodel and a land-cover simulation submodel (Fig. 2). The urban growth submodel simulates the urban land expansion driven by socioeconomic and demographic factors. The land-cover simulation submodel predicts landscape change as the result of urban spatial growth. The simulation is controlled by the spatial choice utility function. Socioeconomic and demographic data, land-cover data of multiple years derived from Landsat remotely sensed images, and multisource GIS data were employed to define the simulation conditions and restrictions.

2.2.1. Spatial units

We created three levels of spatial units: *section*, *compartment*, and *cell* in DLS modeling. A section is the basic spatial unit for the construction of transition structures. It is not to be confused with subunits of the public land survey system. Multiple sections were applied to present variations of land transitions. This separation allowed us to use more than one transition rate in a large area, which overcame the shortcomings of using a sin-

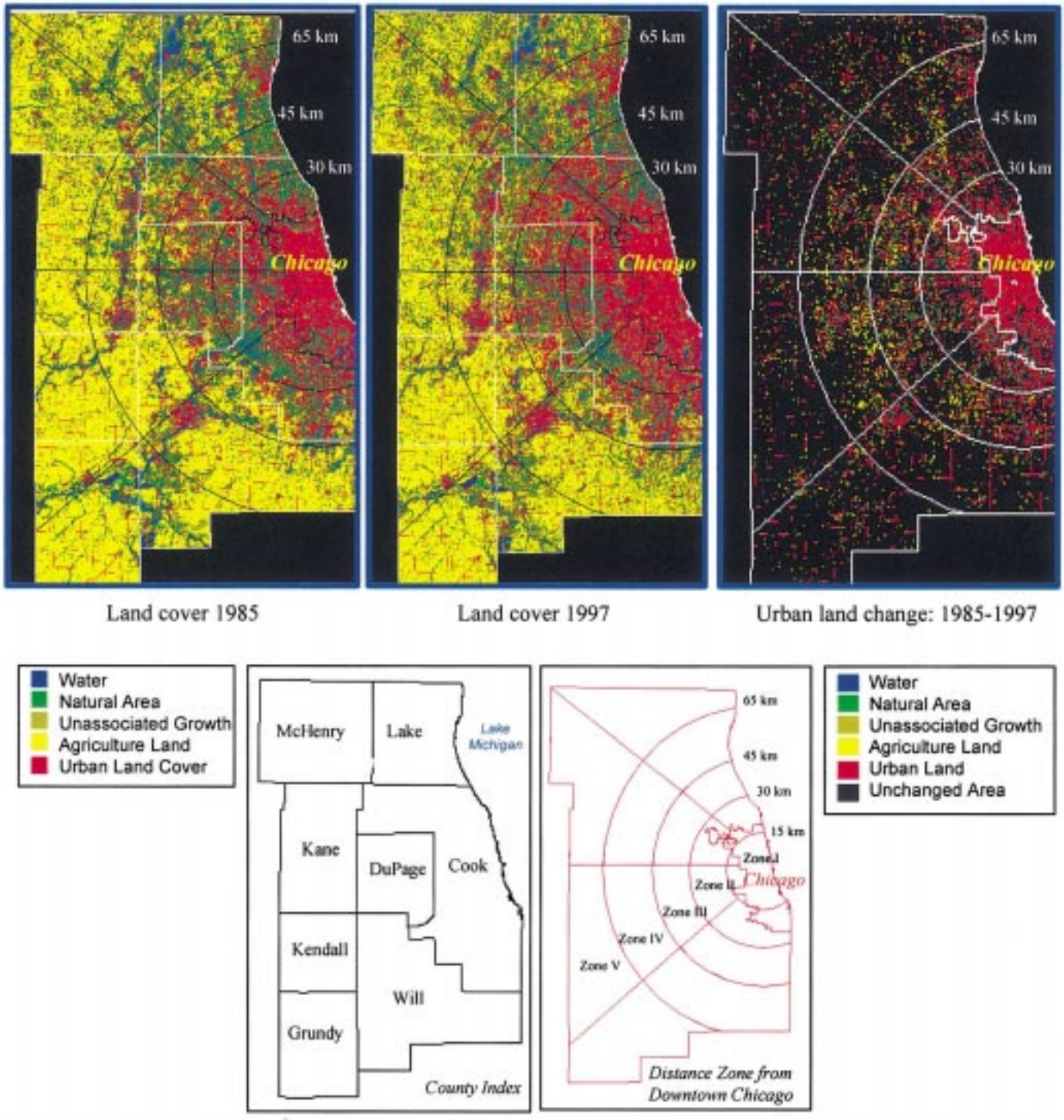

Fig. 1. Land cover of northeastern Illinois in 1985 and 1997, and the land cover changes.

Table 1
Landscape patch density of the Chicago region in 1997

Distance and area of the zones	Natural area (Patches/km^2)	Unassociated growth (Patches/km^2)	Agriculture land (Patches/km^2)	Urban land (Patches/km^2)
Zone I (0–15 km, 473.92 km^2)	0.93	1.12	0.33	1.9
Zone II (15–30 km, 1187.65 km^2)	2.65	2.94	0.62	3.38
Zone III (30–45 km, 1768.19 km^2)	4.05	2.9	1.41	3.36
Zone IV (45–65 km, 3335.43 km^2)	3.9	2.5	2.26	2.81
Zone V (>65 km, 4887.67 km^2)	3.39	2.32	2.58	2.19

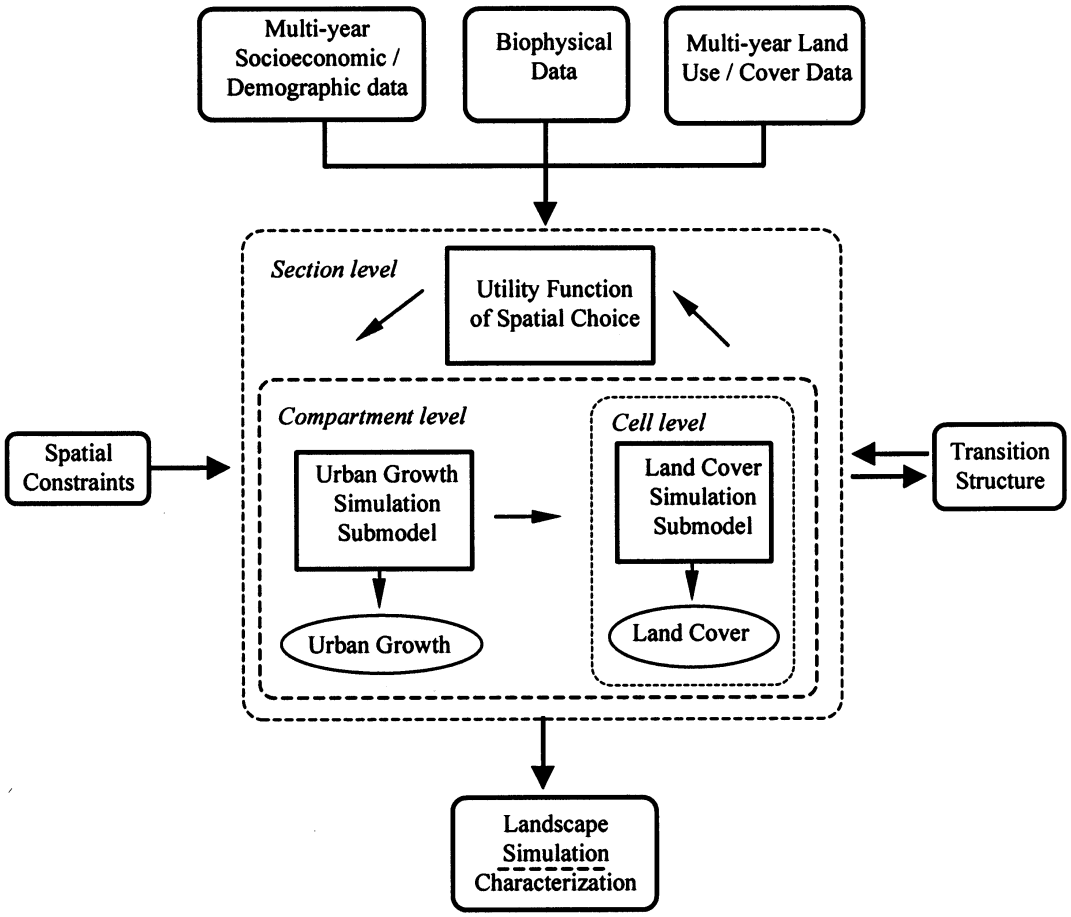

Fig. 2. The DLS model takes multi-year socioeconomic and demographic data, biophysical data, and multi-year land-cover data as input. Urban growth simulation submodel and land-cover simulation submodel are integrated using utility function of spatial choice. Spatiotemporal interaction between two submodels is achieved by three levels of spatial units, i.e. section, compartment, and cell. The simulation is controlled by dynamic transition thresholds and rates, spatial constraints, and socioeconomic/demographic driving factors. The model output represents a dynamic series of landscape simulations.

gle transition rate to simulate the landscape of the entire region. Spatial location and landscape characters of the region were referenced to design the eight sections for the study area (Fig. 3).

Table 2
Urban land-cover changes of the study area, between 1985 and 1997, by zones

Land cover change	Nature to urban (ha.)	Unasso. growth to urban (ha.)	Agriculture to urban (ha.)	Urban land in 1985 (ha.)	Urban land change (%) 1985–1997	Urban change density (ha./km^2)
Zone I	329	295	149	38 059	2.03	1.63
Zone II	3559	3232	1335	48 037	16.92	6.84
Zone III	5505	7479	7428	32 917	62.01	11.54
Zone IV	5049	7663	10 044	29 898	76.11	7.26
Zone V	1739	4896	6035	23 992	52.81	4.04

Compartments, 2.5×2.5 km areas within sections, are the second level spatial unit. They control the spatial step of the simulation for the urban growth submodel. Each compartment possesses a set of state variables. The state variables are constant at a given model iteration. Urbanized area in each compartment is calculated at a given time interval Δt based on the initial state condition at time t. The change of urbanized land, as a new state variable of the compartment, represents a driving factor in landscape change. The size of the compartment was determined by referencing the mean size of the polygons that represent the 270 municipalities of the Chicago metropolitan region.

The cell, sized at 150×150 m (5×5 Landsat TM pixels), is the minimum spatial unit in the DLS model. A cell reflects the land-cover status at a given time in this spatial unit. Under the control of the expected urbanized area within each compartment at time $t + \Delta t$, the states of cells at $t + \Delta t$ are simulated. Cells within different compartments have different controls for their expected urban land areas. Changes of a cell's land-cover types alter the state variable of the compartment.

2.2.2. Urban growth simulation submodel

The urban growth simulation submodel is a key to bridging the human driving factors and landscape change. Only when urban growth can be effectively modeled can the impacts of population and employment increase on landscapes be accurately simulated. Therefore, an urban growth simulation was designed as a submodel in this DLS approach. The concepts of effective population, utility and marginal utilities, construction of utility function, and using these concepts in urban growth simulation are discussed as follows.

2.2.2.1. Effective population. In this study, urban land consumption is considered as residential-, commercial- and industrial-related land uses. Ef-

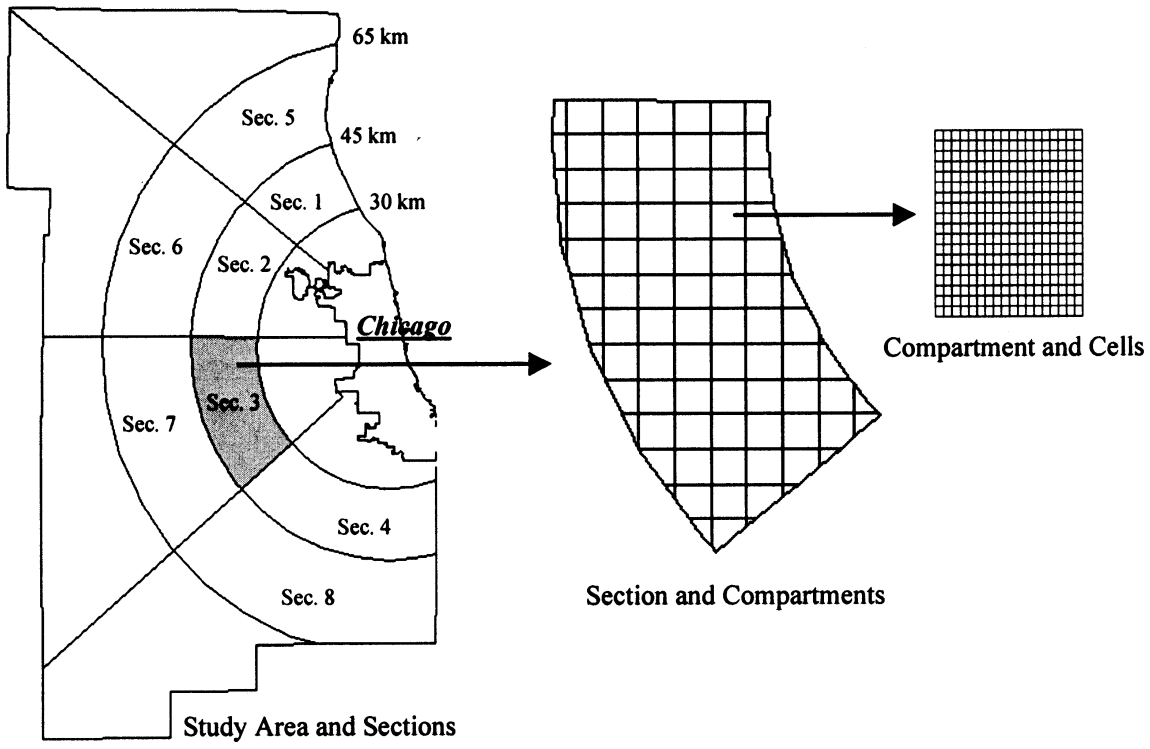

Fig. 3. Study area and the spatial units. Section is the basic spatial unit that is applied to construct transition structures; Compartment is the basic spatial unit for urban growth submodel. Compartment is 2.5×2.5 km in size. Cell is the minimum spatial unit for land-cover simulation submodel. Cell is 150×150 m in size and contains 5×5 Landsat TM pixels.

fective population (P_{eff} is defined as the sum of residential population (P_{resi}) and weighted number of employment (P_{empl}) in a given spatial area. Square kilometer is applied as the given spatial area.

$$P_{eff} = P_{resi} + R\,P_{empl}. \quad (1)$$

P_{resi} and P_{empl} are the hosts that consume residential as well as commercial and industrial land uses. P_{eff} reflects human effects on consumption of land by the above land uses. P_{resi} and P_{empl} can be obtained from census and employment data. In order to calculate effective population, the R (Eq. (1)) is used to transform the number of employment to the weighted number of employment. R is the ratio between average urbanized areas occupied by residential and by employment in each section.

2.2.2.2. Spatial choice and the utility function. Theoretical studies of applying spatial choice utility functions have been documented (Timmerman and Borgers, 1989; Leonardi and Papageorgiou, 1992). In this study, spatial choice is a process in which effective population compares the attributes of the compartments within a feasible set of choices and chooses the most probable compartment to occupy. Urban growth represents an expansion of urban land-use that associates with spatial choice of effective population. We define utility as a measure that the effective population derives from the attributes within the selected compartments. A utility function, therefore, represents a relationship between the quantities of the attributes of compartments that the effective population occupies and the utilities derived from the attributes. Each compartment has a utility value. The utility functions are employed to derive probabilities of the compartments that are to be occupied by effective population.

A section of the study area is divided into a set of compartments. Spatial location of a compartment is described by its central coordinates of $z = \{(x_1, y_1), (x_2, y_2), \ldots (x_z, y_z\}$, where Z is the total number of compartments. The attribute vector of z is specified as $S(z; t) = \{s_1(z; t), s_2(z; t), s_3(z; t) \ldots s_n(z; t)\}$, where n is the number of dimensions of attribute vectors that describes the features of the compartments. The compartments define a discrete space for the utility function of spatial choice. Spatial choice of the ith socioeconomic element is described by utility function as:

$$U^i(z; t) = f[S(z; t), H^i(t)] + \varepsilon(t) \quad i = 1, 2, 3 \ldots m)$$
$$(z; t) \in (Z; t) \quad z = \{(x_1, y_1), (x_{2,}\, y_2), \ldots, (x_z\, y_z)\} \quad (2)$$

where:

$U^i(z;\ t)$: is the utility function associated with spatial choices of location z ($z = 1, 2, 3, \ldots Z$) by the ith socioeconomic element at time t;
$S(z;\ t)$: is the attribute vector of compartment z at time t;
$H^i(t)$: is the characteristic of the ith socioeconomic element at time t;
$\varepsilon(t)$ is the random disturbance at time t;
$(Z; t)$: is the set of locations that have the potentials to be selected by the ith socioeconomic element at time t;
$Z = (x; y)$: is a geometric central coordinate of the spatial compartment z;
m: is the total number of socioeconomic elements considered.

In the model, spatial choice depends on two factors: landscape pattern ($S(z; t)$) and characteristics of socioeconomic elements ($H^i(t)$). Human activities as one component of spatial choice can be represented by a utility function.

2.2.2.3. Construction of the utility function. To construct a utility function, we assume that the spatial distribution of effective population obeys a utility function of spatial choice. If $P(z)$ is the change rate of the density of effective population, U is the utility function associated with spatial choice of location by effective population, then

$$P_z = C\,U(k_1, k_2, \ldots, k_n), \quad (3)$$

where C is a constant and can be defined as the ratio of the change rate of effective population

and the utility value. It can be derived during the construction of utility functions. The k_is represent the ith attributes that impact spatial choices of effective population. The attributes considered include: (1) density of effective population; (2) employment in a given compartment; (3) road density; (4) degree of facility accessibility (Flamm and Turner, 1994); (5) degree of transportation accessibility which is the time-distance to major transportation; and (6) proportion of non-urban land in each compartment. All six attributes were normalized to a range of 0–100.

To implement the above discussion, a utility function needs to be constructed for each of the above attributes k_j ($1 \leq j \leq n$, $n = 6$) by finding a set of compartments which possess constant attributes for all k_i ($i \neq j$). Then k_j is the only attribute that alters the changing rate of the density of effective population.

In order to construct a utility function, a marginal utility needs to be defined. A marginal utility is the increment of utility caused by the unit increase of certain attribute (Peterson, 1989). The marginal utility $M_u(k_{jl})$ is defined as:

$$M_u(k_{jl}) = \frac{1}{C}\frac{\Delta P_l}{\Delta k_{jl}} \quad (l = 1, 2, \ldots L), \tag{4}$$

where L is the number of compartments in the selected set. Δk_{jl} is the increment of the influence factor. ΔP_l is the increment of changing rate of the density of effective population caused by the changes of the influence factor. A curve-fitting process can be applied to explore the relations between influence factor k_j and the change rate of the density of effective population. Let $M_u(k_j)$ be the fitting curve function, the utility of k_j is:

$$U(k_j) = \int_0^{k_j} M_u(k_j)dk_j. \tag{5}$$

Since the K_j has been normalized to a continuous variable between 0 and 100, the influencing impact of K_j can be quantified. Following the same process, utility functions for other influence factors, $U(k_1)$, $U(k_2)$ … $U(k_n)$, can be derived. By the additive rule of utility (Mansfield, 1982), the total utility function of spatial choice for effective population is derived as:

$$U[k_1(x, y), k_2(x, y), \ldots k_n(x, y)] = \sum_{i=1}^{n} U[k_i(x, y)]. \tag{6}$$

The following example explains the methodology for constructing a utility function for the attribute $U(k_6)$ the proportion of non-urban land. The utility function in this example was derived for section 6 (Fig. 3). Applied data included: employment and residential data in 1985 and 1996, land cover data in 1985 and 1997, and road density. The influence factors of k_j ($j = 1, 2, \ldots, 6$) and the $P(z)$ between 1985 and 1997 for the 255 compartments within this section were derived from the above data. Seventy-six compartments that had the same influence factors of k_1 through k_5 but different k_6 were selected. Therefore $L = 76$. The change rate of $\Delta P(z)/\Delta k_{61}$ ($l = 1, 2, \ldots, 76$) was calculated. For each k_{61}, a corresponding $\Delta P(z)/\Delta k_{61}$ was observed. The relationship between k_{61} and $\Delta P(z)/\Delta k_{61}$, which represented the marginal utility value of k_{61}, was computed (Fig. 4a). According to the law of diminishing marginal utility (Sher and Pinola, 1981; Mansfield, 1982; Peterson, 1989), the additional utility derived from the consumption of an additional quantity of an attribute in the compartments should decrease. Therefore, the fitting curve of this relationship was expressed as an exponential relationship:

$$M_u(k_6) = A \exp(B k_6), \tag{7}$$

where A and B are constants which can be determined by the 76 pairs of k_{61} and $\Delta P(z)/\Delta k_{61}$. The marginal utility function was derived (Fig. 4b). From the marginal utility function the constructed utility function for the influence factor k_6 in the selected section was obtained (Fig. 4c).

2.2.2.4. Simulating urban growth. A compartment and a given iteration of the model are the basic spatio-temporal units for the simulation of urban growth. In this study, time interval Δt was applied as the time break in which the state of variables would be adjusted. Every 5 years starting from 1997 was defined as a time interval. An initial state of the attributes for each of the compartments was obtained from multiple GIS data and census data. In each iteration, the attributes and

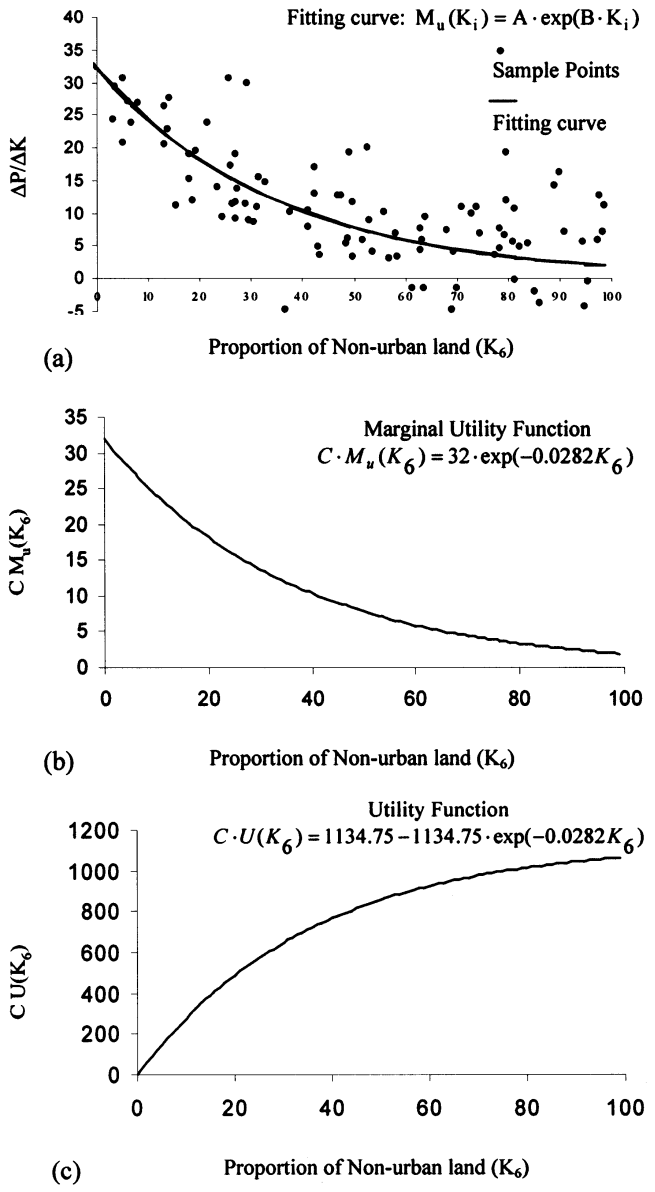

Fig. 4. The process for constructing a utility function. (a). Relationships between proportions of non-urban land attribute (k_6) and the ($\Delta P/\Delta k_6$); (b) marginal utility function; (c) utility function.

utility values were calculated. Newly added effective population in each section was allocated by Eqs. (8) and (9).

$$\Delta P^S(i, t+\Delta t) = \Delta P^S(t+\Delta t)\, e^{U^{S(i,t)}} / \sum_{i=1}^{n} e^{U^{S(i,t)}} \quad (8)$$

$$A_m^S\, \Delta P^S(i, t+\Delta t) \le A_a^S(i, t), \quad (9)$$

where $\Delta P^S\ (i, t+\Delta t)$ is the increment of effective population within the ith compartment of the Sth section in a given time interval Δt. $\Delta P\ (t+\ \Delta t)$ is the increment of effective population within the Sth section in a given time interval Δt. $U^S\ (i, t)$ is the utility of the ith compartment within the Sth section at time t. A_m^S is an average urban area for each unit of effective population. $A_a^s\ (i, t)$ is the available land within the ith compartment of the Sth section at time t for urban expansion. The available land was extracted from land cover data by excluding the areas of restrictions. The areas of restrictions include nature preserves, flood zones, buffered areas around urban constructions and major road networks, and other areas that are very unlikely to be consumed by urbanization, such as water surface and wetland sites. The constant C in the utility function was obtained when the allocated population (Eq. (8)) best approximated to the distribution of census population. A search algorithm that applied the rule of minimum of quadratic sum of residual was developed to obtain the C. If there is no available land in one compartment, the unallocated effective population will be reallocated to the neighboring compartments (Eq. (9)). In each model iteration, at first, the increment of effective population $\Delta P^S\ (i, t+\Delta t)$ is allocated (Eq. (8)). If $A_m^S\ \Delta P^S\ (i, t+\Delta t) \le A_a^S\ (i, t)$, the allocation process stops. Otherwise, unallocated effective ΔP_r^i in the ith compartment is calculated and reallocated into neighboring compartments (Fig. 5). Cross section reallocation of effective population is applied when there is no available land within one section. The expected urban land ($A_e(i, t+\Delta t)$) for each compartment is derived by

$$A_e(i, t+\Delta t) = A^S\, \Delta P^S\ (i, t+\Delta t). \quad (10)$$

2.2.3. Land cover simulation submodel

Transition potentials and thresholds, and urban growth simulation are the keys that affect the results of landscape simulation. The density of effective population and the proportion of non-urban land cover are the two attributes that bridge the urban growth simulation submodel and the land-cover simulation submodel. These two attributes dominate the interactions of the two submodels. Expected urbanization is obtained by Eqs. (8)–(10). The urbanization controls land-

cover simulation. The results of land-cover simulation alter the influencing factors that contribute to the utility functions (Eq. (6)).

2.2.3.1. Spatial distribution of transition potential. Transition potential represents the possibility of state change for a cell from current land-cover type to other categories. Transition potential is a function of its current land-cover type, the land-cover types of its neighboring cells, and average transition rate of the section. In this study, a 3×3 moving window was used to the 8 referenced neighboring cells. The transition potential is expressed as:

$$PC^m(c_i, c_j, S, t+\Delta t) = NC^m(c_j, t)\ Tr(c_i, c_j, S, t)/8, \quad (11)$$

where $PC^m\ (c_i, c_j, S, t+\Delta t)$ is the transition potential for the mth cell in the Sth section which changes from type c_i to c_j from time t to $t+\Delta t$. j is the number of all possible land-cover types. $NC^m(c_j, t)$ is the total number of cells among the 8 neighboring cells that possess the same land-cover type of c_j at time t. $Tr(c_i, c_j, S, t)$ is the transition rate from c_i to c_j at time t within the Sth section.

2.2.3.2. Spatial distribution of transition threshold. Transition thresholds (TH) are boundary values of transition potentials. The transition of state for a cell will possibly take place when its transition potential is greater than the boundary value. In this study, a transition threshold was derived for each transition option. A matrix of transition thresholds was applied for each section. The matrices of transition thresholds were calculated from multi-year land covers derived from remotely sensed data. The search algorithm for

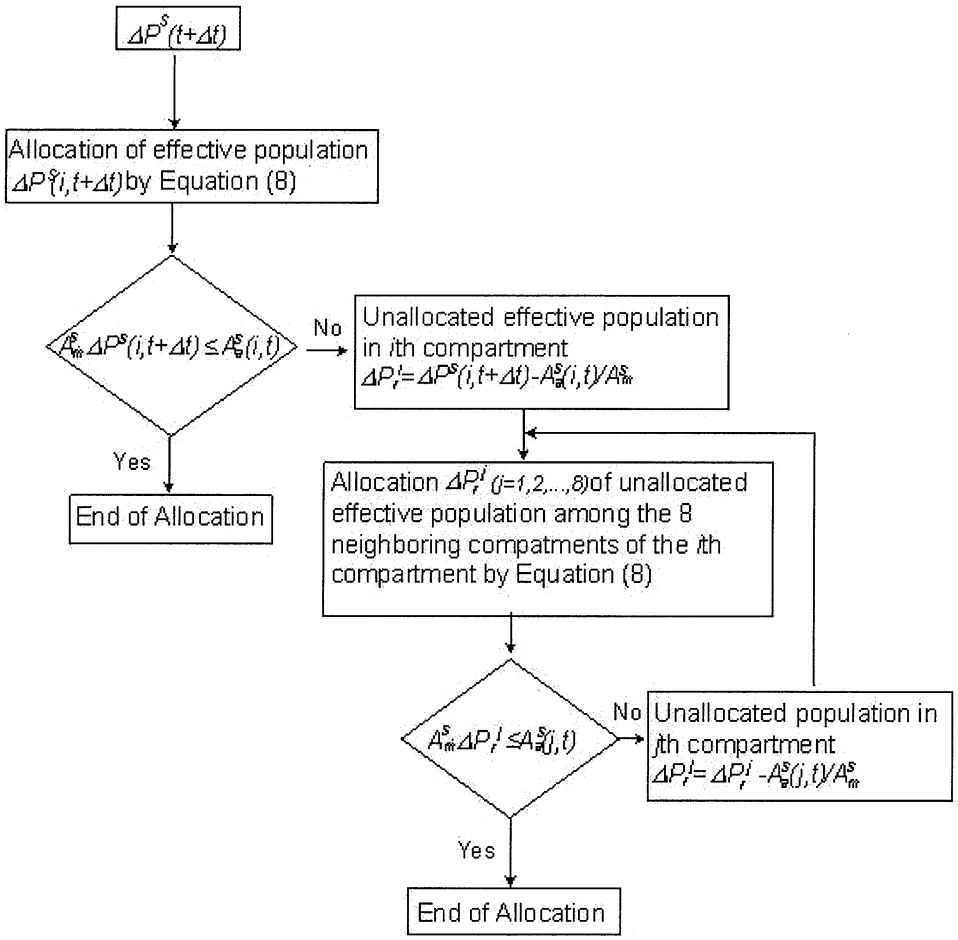

Fig. 5. The process of allocation of effective population.

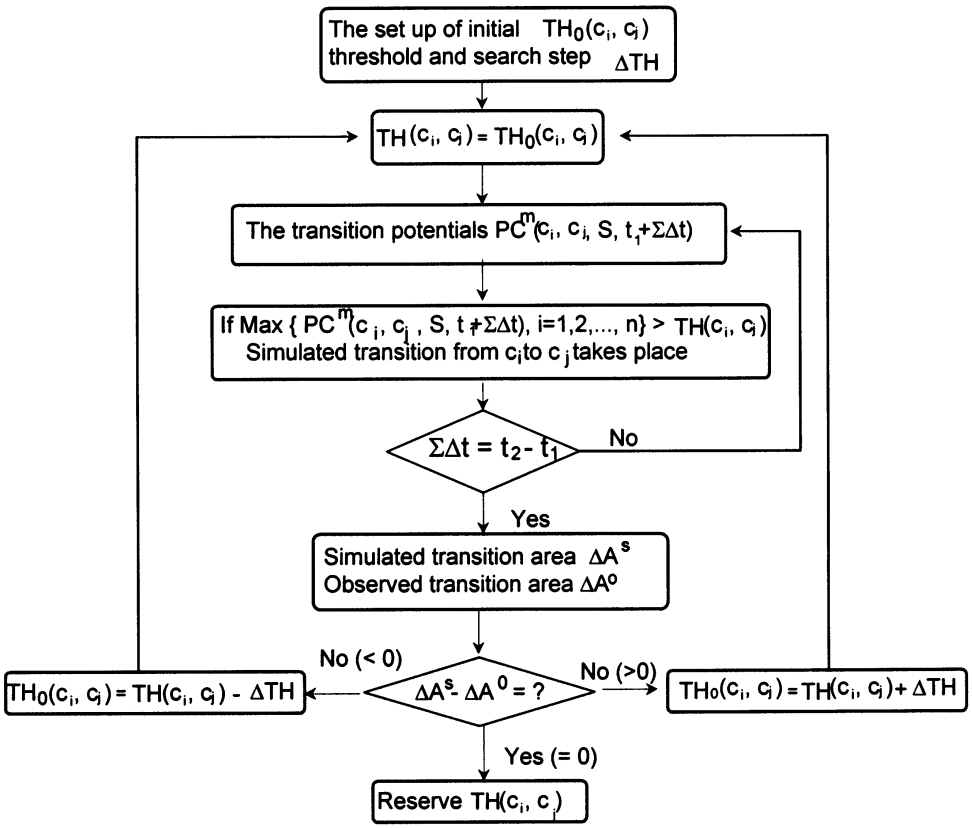

Fig. 6. Search algorithm for obtaining transition threshold (TH).

transition thresholds among non-urban land-cover categories was designed (Fig. 6).

The search process for $TH(c_i, c_j)$ began by setting up both an initial threshold $TH_0(c_i, c_j)$ and a search step ΔTH. The initial threshold was developed subjectively by referencing the characteristics of land-cover changes in the study area. During each model iteration Δt, transition potentials of all cells PC^m $(c_i, c_j, S, t + \Sigma\Delta t)$ were calculated. $\Sigma\Delta t$ was the accumulation of time steps within the time interval of $t_2 - t_1$ The transition potential for each cell was examined. If

$$\max [PC(c_i, c_j, S, t + \sum \Delta t), i = 1, 2, \ldots, n\} > TH(c_i, c_j), \quad (12)$$

a simulated change for the cell from c_i to c_j would take place. When $\Sigma\,\Delta t = t_2 - t_1$, the simulated transition area (ΔA^S) and observed transition area (ΔA^O) were obtained. The (ΔA^O) was observed from land covers derived from historical remotely sensed data. When $(\Delta A^S \approx \Delta A^O)$, the $TH\,(c_i, c_j)$ was reserved for further use; if $(\Delta A^S > \Delta A^O$, $TH_0(c_i, c_j) = TH(c_i, c_j) + \Delta TH$; if $(\Delta A^S < \Delta A^O$, $TH_0(c_i, c_j) = TH(c_i, c_j) - \Delta TH$, and the new search of $TH(c_i, c_j)$ began. This process continued until the set of thresholds was obtained for all sections.

2.2.3.3. Impact simulation of urban growth on land cover change. In each time interval Δt, the urban growth submodel simulated the expected urban land $A_e(i, t + \Delta t)$ for each of the compartments. The transition threshold from non-urban to urban land was searched under the control of expected urban land at time $t + \Delta t$. The following controls were applied to simulate land-cover change for cells: (1) the transition threshold from non-urban to urban land for each of the compartments; (2) the transition threshold among non-urban land-cover types for each of the sections; and (3) the expected urban area for each of the compartments.

2.2.3.4. Land cover simulation. Remote sensing derived land-cover data at a given time (e.g. 1997) were set up as the initial state for the land-cover simulation. We calculated the total number of cells among 8 neighboring cells which possessed the land-cover type of c_j at time t, $PC^m(c_i, c_j, S, t+\Delta t)$, and the transition potential for the mth cell in the Sth section which changed from type c_i to c_j from time t to $t+\Delta t$. If c_j was in the urban land category, the transition threshold was calculated by a loop searching each compartment. The process was controlled by expected growth of urban land (Eq. (10)). If the c_j was other land-cover type rather than urban, the obtained threshold $TH(c_i, c_j)$ applied.

Spatial restrictions for urbanization were applied. If a cell fell into a restricted area, the transition to urban land cover would not take place. Transitions among other non-urban land-cover types were possible. However, transition from natural area to agriculture land-use was precluded. If

$$PC^m(c_i, c_j, S, t+\Delta t) > \max\{PC^m(c_i, c_l, S, t+\Delta t), i=1, 2, \ldots, n, l \neq i, l \neq j\} \quad (13)$$

and

$$PC^m(c_i, c_j, S, t+\Delta t) > TH(c_i, c_j), \quad (14)$$

then, the transition from c_i to c_j would take place. The process continued until the simulation for all the sections was completed for the given time interval.

2.3. Landscape simulation and analysis methods

Landscape simulation and characterization were organized in GIS environment. Arc/Info 8.01 (Environmental Systems Research Institute, Redland, California, USA) and ERDAS Imagine 8.4 (ERDAS, Inc., Atlanta, Georgia, USA) software systems, AML (Arc Micro Language) and C programming were employed to implement the model.

2.3.1. Data source

Primary data sources applied in this study include: (1) land-cover data of 1972, 1985, and 1997, which were derived from classification of October 1972 Landsat Multispectral Scanner (MSS) data and May 1985 and October 1997 Landsat TM data; (2) 1980 and 1990 census data from the U.S. Bureau of the Census; (3) estimated population, household, and employment data for 1996 from NIPC (1998); (4) projected population, household, and employment data of northeastern Illinois for the year 2020 from NIPC (1998); and (5) GIS spatial and attribute data of municipalities, transportation, flood zones, and nature preserves. In the projected demographic and employment changes, NIPC considered that the actual future levels and distributions of population and employment would be the result not only of countless private sector decisions but also of important government policy and investment actions. The forecast did not suggest a continuation of past development patterns. Instead, the forecast was based on the expectation that public policy and investment would give increased emphasis to the maintenance of existing communities, revitalization of declining areas, and cost-effective and environmentally-sensitive new development (NIPC, 1998). We assumed that the above considerations were applied when we used the NIPC's forecast data in urban growth and landscape simulations.

2.3.2. Extraction of land cover information and the transition rate

To extract land-cover information for 1972, 1985, and 1997, Landsat images of these years were rectified and georeferenced to the Universal Transverse Mercator (UTM) coordinate system. Supervised classification using a maximum likelihood classification algorithm of the ERDAS Imagine system was employed to classify the images. Land-cover types included woodland, savanna, prairie, wetland, unassociated growth, agriculture, and urban land. Unassociated growth represented the areas created by human disturbance. Original natural communities had been destroyed. Secondary trees and shrub growths were the dominant features of unassociated woody growth. Unassociated grassy areas included prairie restoration sites that had been recovered from formerly agricultural tracts.

Intensive fieldwork was conducted to assist training-signature selection, using GPS to accurately position ground truth. The GPS positioning data were differentially corrected, projected to the UTM coordinate system, and converted into GIS coverage in Arc/Info vector format. Using ground truth, 132 training signatures of natural and cultural land-cover categories were defined to classify the 1997 TM image. To assist in the classification of 1972 and 1985 Landsat data, multisource spatial data were referenced. These included historical air photos; land-use and land-cover maps of the region developed in 1974 and 1990, ecosystem maps and management records from the forest preserve and conservation districts in each of the northeastern Illinois counties; and USGS topographic maps. A total of 145 and 87 training signatures for land-cover categories were defined by their spectral characteristics to classify the 1985 and 1972 Landsat data, respectively.

To simplify the DLS modeling conditions, generalization was applied during post-classification process to recode classified land-cover data into five general land cover types, i.e. water, nature area unassociated growth, agriculture, and urban land. Assessment of classification accuracy for the generalized land cover shows that about 93% overall accuracy was achieved for the 1985 and

Table 3
Confusion matrix of classification of May 1985 Landsat TM data

	Classified data						
	Natural area	Unassociated growth	Agriculture land	Urban land	Row total	Omission error (%)	Accuracy (%)
Reference data							
Natural area	201	6		1	208	3.36	96.63
Unassociated growth	40				40	0	100
Agriculture land			52	6	58	10.34	89.66
Urban land	7	8		100	115	13.04	86.96
Column total	208	54	52	107	421		
Commission error (%)	3.36	25.92	0	6.54			Overall 93.35%

Table 4
Confusion matrix of classification of October 1997 Landsat TM data

	Classified data						
	Natural area	Unassociated growth	Agriculture land	Urban land	Row total	Omission error (%)	Accuracy (%)
Reference data							
Natural area	248	6	3	1	258	3.88	96.12
Unassociated growth		53	2	2	57	7.02	92.98
Agriculture land	1	1	60		62	3.23	96.77
Urban land	2	8	3	92	105	12.38	87.62
Column total	251	68	68	95	482		
Commission error (%)	1.98	22.06	11.76	4.17			Overall 93.98%

Table 5
Transition rate in sections among land cover categories between 1972 and 1997

	Nature	Unasso. G.	Agri.	Urban
Section 1				
Nature	0.570	0.105	0.011	0.138
Unasso. G.	0.239	0.253	0.030	0.303
Agri.	0.016	0.173	0.100	0.523
Urban	0.097	0.077	0.007	0.646
Section 2				
Nature	0.417	0.150	0.022	0.231
Unasso. G.	0.117	0.347	0.036	0.325
Agri.	0.021	0.138	0.142	0.513
Urban	0.064	0.075	0.010	0.679
Section 3				
Nature	0.467	0.166	0.026	0.162
Unasso. G.	0.125	0.353	0.057	0.293
Agri.	0.015	0.137	0.311	0.349
Urban	0.075	0.099	0.020	0.630
Section 4				
Nature	0.440	0.194	0.029	0.154
Unasso. G.	0.108	0.379	0.092	0.246
Agri.	0.037	0.160	0.414	0.209
Urban	0.049	0.101	0.021	0.657
Section 5				
Nature	0.468	0.207	0.040	0.106
Unasso. G.	0.155	0.399	0.077	0.193
Agri.	0.050	0.240	0.300	0.223
Urban	0.071	0.135	0.018	0.601
Section 6				
Nature	0.462	0.225	0.039	0.095
Unasso. G.	0.132	0.437	0.074	0.182
Agri.	0.068	0.203	0.371	0.175
Urban	0.076	0.152	0.031	0.562
Section 7				
Nature	0.287	0.270	0.080	0.181
Unasso. G.	0.069	0.379	0.149	0.228
Agri.	0.024	0.106	0.566	0.127
Urban	0.037	0.104	0.024	0.658
Section 8				
Nature	0.379	0.263	0.069	0.109
Unasso. G.	0.085	0.405	0.196	0.143
Agri.	0.033	0.148	0.596	0.052
Urban	0.032	0.142	0.039	0.614

1997 data (Tables 3 and 4). The 1972 land-cover data was achieved by classification of MSS data. Although the spatial resolution of MSS (79 m) was different from TM (30 m), the coarser data represented the land-cover patterns in 1972 well. A 88% overall accuracy was achieved for the 1972 land-cover data. The classifications of the Landsat data quantified land-cover types for the above years and revealed change patterns of the region.

Transformation of land use from agriculture to urban was evident for the sections in Zone III. Section 1 and 2 possessed the highest transition rates of 0.523 and 0.513, respectively (Table 5). Sections 3, 4 and 5 possessed relatively lower transition rates of 0.349, 0.209, and 0.223. Sections 6, 7, and 8, within the outer ring Zone IV, had no sign of predominant transformation from agricultural to urban land during the same time period. The transition rate from unassociated growth to urban land presented a relatively balanced spatial distribution among the sections in the zone they located. This revealed that the transition rates were unbalanced among the sections or throughout the study area. Therefore, the use of section as one of the spatial units provided more detailed transition estimations for the simulation.

2.3.3. Simulation conditions

The following conditions were applied in DLS simulation. The time period was from 1997 to 2020 with a 5-year interval started at 1997. A 3-year interval was applied from 2017 to 2020. Urban growth and the land cover were simulated for 2002, 2007, 2012, 2017, and 2020. Compartments were used as the spatial unit in urban growth simulation submodel. Cells were used as the spatial unit in land-cover simulation submodel. The broader scale of compartments (2.5×2.5 km) facilitated the construction of utility function of spatial choice which was based on socioeconomic data. On the other hand, the finer spatial unit of cells (150×150 m) allowed the details of land-cover simulation to be conducted. Eight cells centered by the target cell within a 3×3 window were applied for neighborhood-influence analyses. Restricted areas were excluded from the available land for urban growth. The effective population, which is the combined effects of projected increases of employment and human population from 1997 to 2020, was applied as the main driving factor in urban growth and land-cover change.

2.3.4. Landscape characterization

Landscape indices of 'patch number', 'patch density', 'average patch size', 'maximum patch size', and 'standard deviation of patch sizes' were used to characterize the regional landscapes. ArcGrid GIS was employed to convert raster land-cover data into a vector GIS coverage prior to the calculation. Arc/Info AML and C programs were developed to calculate the above landscape indices. Quantification of the 1997 landscape revealed that the study area (Zone III and IV) possessed more patches for both natural and urban lands than other zones. There was no overwhelming dominant land-cover category in number of patches and in average patch size. This indicates that landscapes in Zone III and Zone IV are relatively fragmented. The area represents the transitions of landscapes from urban to suburban and to agricultural land. It is expected that trends of increasing population and employment will greatly change the landscape of the study area.

3. Results

To evaluate the DLS performance, this approach was tested by simulating 1997 land cover with 1972 land cover as the initial state. The same simulation conditions and attribute factors discussed earlier were applied. For each of the sections land-cover changes detected from 1972 to 1985, and to 1997 were used as baseline data in the calculation of initial transition rates among the four land-cover types (Table 5). The transitions of land-cover categories in a cell depend on urban growth and dynamic transition structure. During the simulation, transition structures in cells were dynamically adjusted by the interactions between urban growth and land cover simulation submodels. Therefore, transition rates were dynamic for the simulation period. A cell by cell agreement among the changed cells was examined. The comparison was made only for those cells in which the land-cover types changed during the time interval. The changed cells were extracted from both DLS simulation and from remote sensing derived land cover by GIS analysis. Comparisons among the changed cells avoid misleading of the percentage of agreement caused by large numbers of unchanged cells for the time period. A 62.3% overall agreement was achieved. Better percentages of agreement were obtained for sections 1, 2, 7, and 8. Lower percentages of agreement were observed for the other sections (Fig. 7).

The results (Fig. 7) indicated that the DLS approach could be influenced by the degree of complexity of the landscapes. For example, the agricultural landscape was predominant in sections 7 and 8 for the time period between 1972 and 1997. The relatively simple landscape contributed to the better agreement between the simulated and remote sensing-derived land covers. More irregular shaped patches of natural landscape and unbalanced socioeconomic and demographic influences contributed to the relative lower simulation agreement for section 5.

The urban land expansion and the consequent land covers of the study area from 1997 to 2020 were simulated by the DLS. Utility functions were constructed for the six socioeconomic and demographic factors and implemented in the urban growth submodel to depict the influence of the

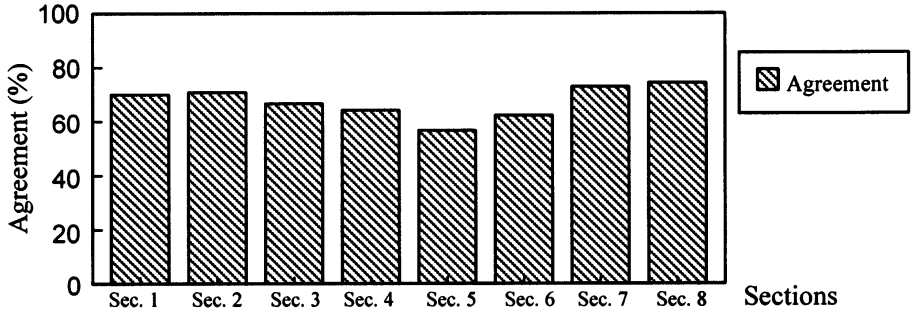

Fig. 7. Agreement between remote sensing-derived and DLS-simulated 1997 land covers among the changed cells.

above factors on the landscape change. The landscape simulations for the years of 2002, 2007, 2012, 2017, and 2020 were achieved (Fig. 8). The simulation indicates that urban growth is evident in the study area. Most agriculture land will be converted into urban land uses by the year 2020. Natural areas tend to be more isolated and surrounded by urban land. The trend of urbanization is predominant particularly for the sections 5, 6, 7, 8 (Fig. 9). Increases in mean patch size, total area, and standard deviation of urban land are evident for all the sections after year 2012.

The comparison of landscape indices among natural and urban areas in 1985, 1997, 2012, and 2020 shows that the total area, the patch density, and the mean patch size of natural areas are in a decreasing trend for all of the sections. The patterns of the patch density and the total area indicate that a major decline of natural areas occurred in sections 1, 2, 3, 4, and 5 between 1985 and 1997. The same trend is continued but at a reduced rate from 1997 to 2020. The lower patch density and smaller mean size indicate that the natural areas in these sections are tending to be more fragmented.

The urban growth increases the number of interfaces between natural and urban landscapes. We used the proportion of interface-edge between two land cover types to characterize the landscape change. The proportions of interface-edge among land cover types show that interface edges shared by natural and urban areas increased from 0.354 in 1972, to 0.368 in 1985, to 0.492 in 1997 (Table 6). The simulated results indicate that the increasing trends of interface-edge between natural and urban areas will continue and reach 0.524 in 2012 and 0.576 in 2020, respectively. The increasing trend of proportion of interface-edge by urban and unassociated growth areas has been observed as well. However, the values of the proportion of interface-edge between natural and unassociated growth areas, and between natural and agricultural areas, are in decreasing trends, mainly caused by consumption of unassociated growth areas and agricultural lands by urban land uses. Although the decrease of patch density and mean patch size of natural areas is not overwhelming (Fig. 9), the changing pattern of the proportions of interface-edge reflects the impacts of human factors on natural areas in the region.

Visual comparison between the patterns of the land covers simulated by the DLS and compiled by the Openlands Project (Openlands, 1999) shows a good match between the two. The Openlands project predicted urban land expansion of the region from year 1998 to 2028 by the information about likely future land patterns obtained through a series of meetings with policy makers, professional planners, open space advocates, builders and developers. Many policy and planning factors, such as sewer-service expansions, highway extensions, and other future infrastructure improvements, were considered. Although the results of the Openlands project were mostly based on the data from qualitative analysis and extensive interviews, the base map upon which the Openlands project findings rooted had been corrected and updated by the most up-to-date development information. Various factors causing development pressures and whether areas would likely develop in the short term (within 10 years) or the long term (from 10 to 30 years) were given full consideration (Openlands, 1999). Visual comparison confirmed that the DLS simulation captured dynamic features of human-induced landscape changes. Since the Openlands project was not GIS-based, no quantitative comparison or measurements between the DLS and Openlands results were attempted.

4. Discussions and conclusions

The DLS approach is designed to integrate urban spatial growth and land-cover change submodels in simulating human-induced landscape change. This integration allows a dynamic adjustment of transition structures during the simulation process. The adjustment overcomes the shortcomings of using a fixed or a constant transition rate. Since human-induced landscape changes are closely related to socioeconomic factors, this adjustment is critical to reflect the spatio-temporal unevenness of human impacts in dynamic modeling. In order to represent the impact, socioeco-

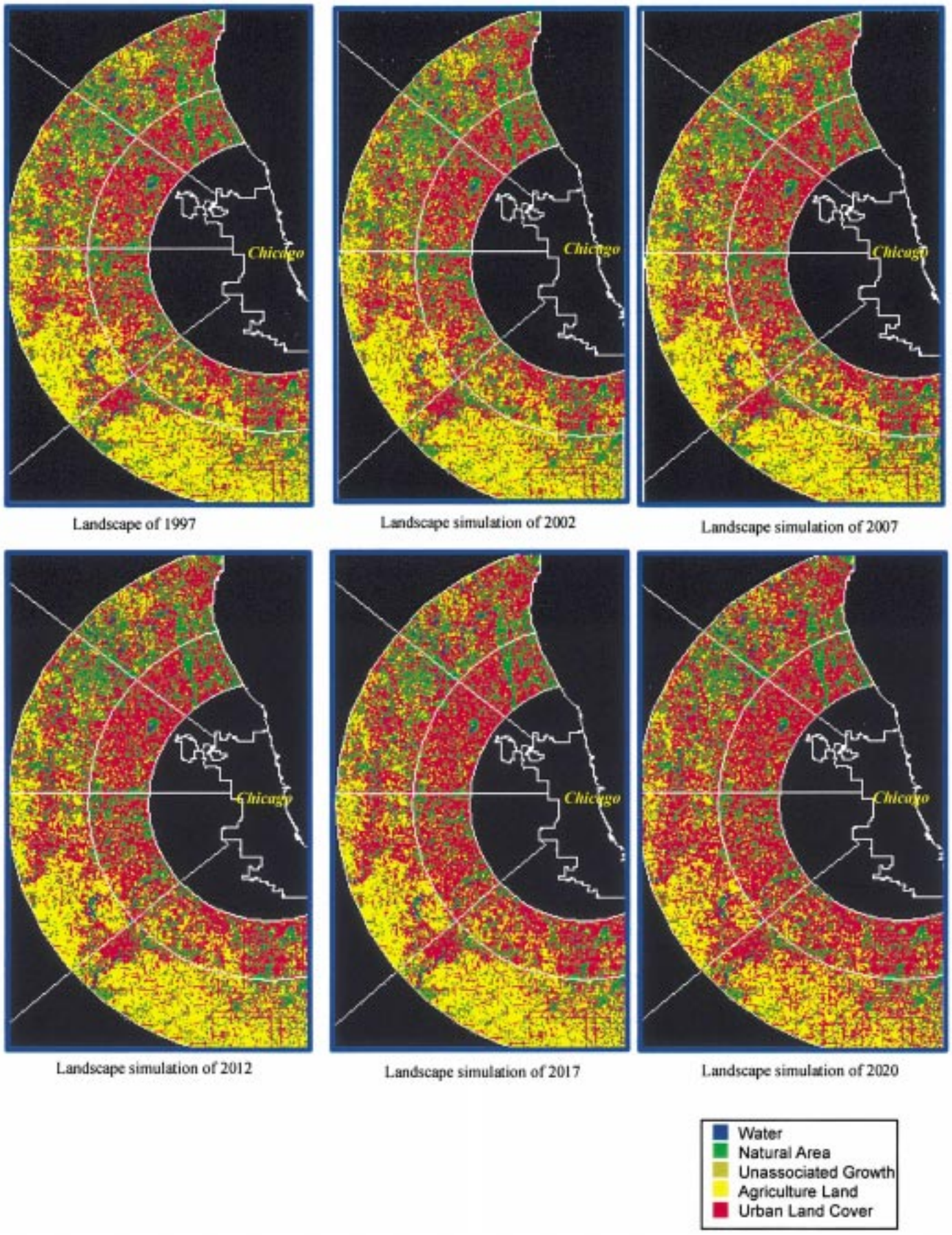

Fig. 8. Result maps of landscape simulation for the selected years from 1997 to 2020.

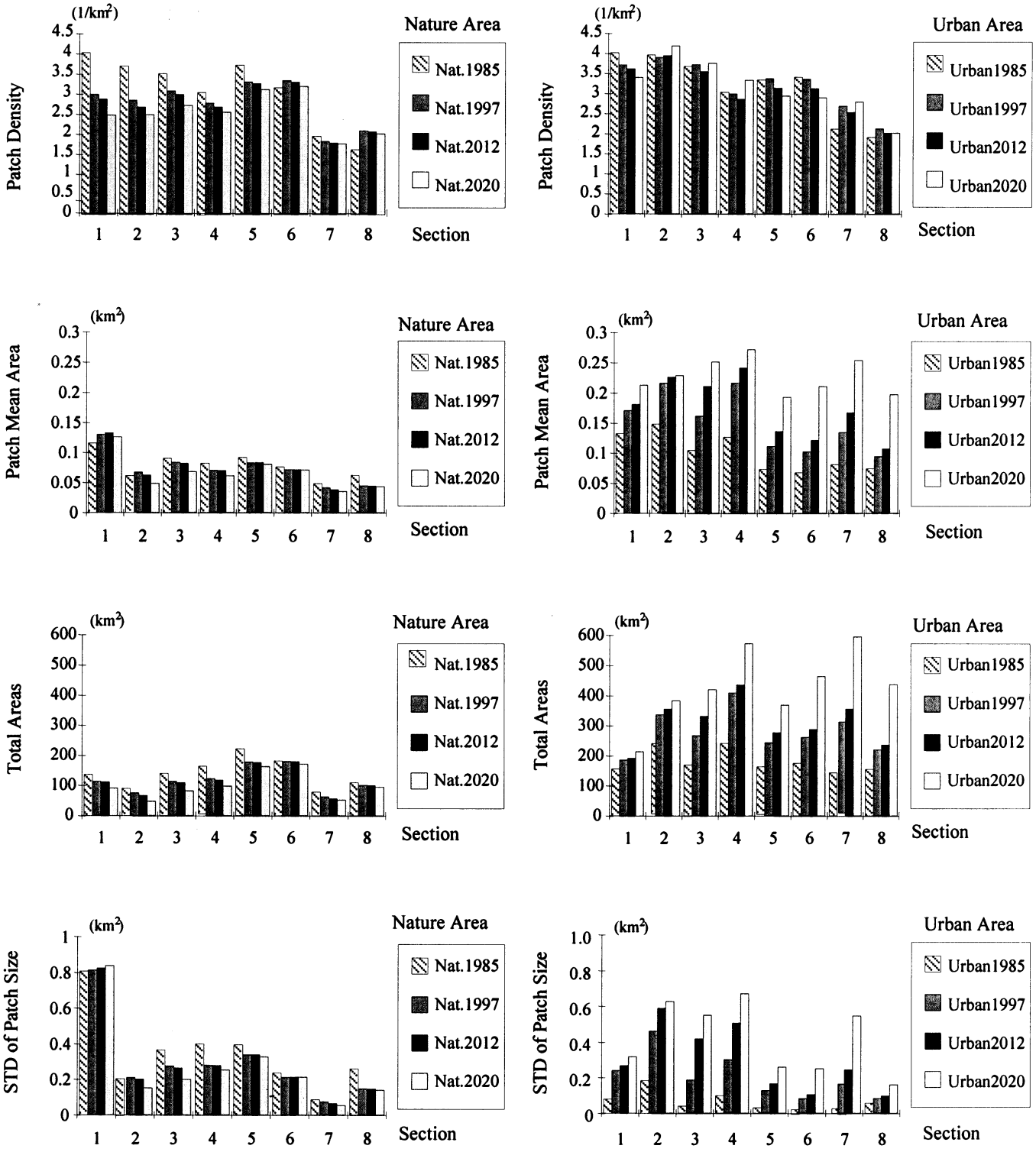

Fig. 9. Comparison of landscape characters by DLS simulated landscape data.

nomic and demographic influences must be treated as internal components of the model. The DLS approach explores a mechanism that can be used to quantify and incorporate human impacts on landscape dynamics. The utility function of spatial choice allows economic principles to be

incorporated into landscape simulation. Although only six socioeconomic and demographic attributes were discussed in this study, the methodology enables the effects of other attributes to be directly linked with the simulation modeling. The methodology in the construction of a utility function creates a new paradigm for building a quantitative model of spatial choice.

Space available for urban land expansion is implicit in DLS, when modeling the spatial demand of urban land and spatial choice of compartments. Spatial restrictions enforced by GIS data can be effectively referenced to limit the areas of available land for urban expansion. Land availability and dynamic change of the attributes within compartments for each time interval, reflect the spatial supply for urban land and adjust the spatial choice of compartment by the effective population for the next time interval.

Multiple spatial units facilitate the interactions among the submodels. The sections allow multiple transition structures to be implemented so that the spatial variance of landscape changes throughout the study area can be represented. This is important particularly when the simulation covers a large area that has unbalanced transition structures and uneven development patterns.

The compartments control spatial scale of urban growth simulation. Compartments adjust transition structures of the sections by dynamic allocation of the effective population. This is the key to incorporate socioeconomic and demographic data into the landscape simulation. Whether the size of the compartment would affect

Table 6
Proportion of interface-edge among land-cover types from 1972 to 1997 and for the simulated years

Land cover category	Nature	Unassociated growth	Agriculture	Urban
Proportion of interface-edge (1972)				
Nature		0.150	0.495	0.354
Unassociated growth	0.255		0.450	0.295
Agriculture	0.399	0.214		0.387
Urban	0.351	0.173	0.476	
Proportion of interface-edge (1985)				
Nature		0.323	0.309	0.368
Unassociated growth	0.310		0.290	0.400
Agriculture	0.312	0.306		0.382
Urban	0.310	0.359	0.325	
Proportion of interface-edge (1997)				
Nature		0.316	0.191	0.492
Unassociated Growth	0.256		0.267	0.476
Agriculture	0.189	0.326		0.484
Urban	0.314	0.374	0.312	
Proportion of interface-edge (2012)				
Nature		0.277	0.199	0.524
Unassociated Growth	0.230		0.259	0.510
Agriculture	0.189	0.294		0.518
Urban	0.312	0.363	0.325	
Proportion of interface-edge (2020)				
Nature		0.231	0.193	0.576
Unassociated growth	0.199		0.244	0.557
Agriculture	0.177	0.258		0.565
Urban	0.313	0.350	0.337	

the simulation result has not been examined yet. It was observed, however, that most of the municipalities in the outer ring areas (>45 km from downtown Chicago) are relatively small in size and had been expanded dramatically in the past 10 years by the annexation of the surrounding available lands. These municipalities have greater potentials to be further expanded. Therefore, the policy of land annexation in northeastern Illinois, as one of the driving factors, can be incorporated into the DLS to improve modeling performance.

The cells, with finer spatial scale, control the spatial step of land-cover simulation. The cell size was designed to bridge the size of a Landsat TM pixel and the spatial scale of the compartment. The cells will facilitate the integration of remote sensing data and the derivatives of land cover with data from other sources. Although the cell is the minimum spatial unit, land-cover type for each of the TM pixels provides sub-cell information that can be applied to refine land cover simulation. Finer resolution of spatio-temporal data in both socioeconomic and biophysical categories should improve and enhance the capacity of the model.

The results of this DLS modeling are particularly telling in the case of one of the most severe threats to the region's environment: urban sprawl and its consequences. The simulated landscapes reveal a dramatic trend in urban land increase. Fragmentation and isolation of the natural communities are evident in the study area and throughout the region. Even though most of the region's high quality natural areas are in conservation management and more open lands will be protected, the integrity and viability of natural ecosystems will be altered by the accelerated transition of surrounding agricultural land to urban structures. The pattern of sprawling growth in the Chicago region has been recognized by the concerned agencies. Region-wide planning efforts, as addressed in the latest regional Biodiversity Recovery Plan (Chicago Wilderness, 1999), are underway. The DLS approach provides a new prototype for this type of regional study. The simulation results are helpful in understanding the current and future landscape patterns and in management planning.

Acknowledgements

We are very grateful to Dr Jianguo Liu of Michigan State University for his detailed advice on improvement of the manuscript. We thank the anonymous reviewers for their insights and critical review of the manuscript. This research was supported by National Aeronautics and Space Administration grants GP37J and NAG5-8829. The land-cover change detection project (NASA Grant GP37J), upon which the land cover data came from, was the collaborative effort of an enormous group of ecologists and land managers in the Chicago metropolitan region and Chicago Wilderness. We thank all of them, in particular Debra Moskovits, Stephen Packard, Wayne Lampa, and Wayne Schennum, for their expertise and insights. We also thank Professor Clifford Tiedemann of the University of Illinois at Chicago for his editorial comments on the manuscript.

References

Boerner, R.E.J., DeMers, M.N., Simpson, J.W., Artigas, F.J., Silva, A., Berns, L.A., 1996. Markov Models of inertia and dynamic on two contiguous Ohio landscapes. Geographical Analysis 28, 56–66.

Chicago Wilderness, 1999. Biodiversity Recovery Plan, Chicago Wilderness, Chicago, pp. 18–26.

Childress, W.M., 1997. Predicting dynamics of spatial automata models using Hamiltonian equations. Ecological Modelling 96, 293–303.

Clarke, K.C., Gaydos, L.J., 1998. Long term urban growth prediction using a cellular automaton model and GIS: Applications in San Franciso and Washington/Baltimore. International Journal of Geographical Information Science 12, 699–714.

Dunn, C.P., Sharpe, D.M., Guntenspergen, G.R., Steams, F., Yang, Z., 1990. Methods for analyzing temporal changes in landscape pattern. In: Turner, M.G., Gardner, R.H. (Eds.), Quantitative Methods in Landscape Ecology. Springer, New York, pp. 173–198.

Ehrlich, P.R., 1988. The loss of diversity: cause and consequences. In: Wilson, E.O. (Ed.), Biodiversity. National Academy Press, Washington, DC, pp. 21–27.

Flamm, R.O., Turner, M.G., 1994. Alternative model formulations for a stochastic simulation of landscape change. Landscape Ecology 9, 37–46.

Gardner, R.H., Milne, B.T., Turner, M.G., O'Neill, R.V., 1987. Natural models for the analysis of broad-scale landscape pattern. Landscape Ecology 1, 19–28.

Hall, F.G, Strebel, D.E., Sellers, P.J., 1988. Linking knowledge among spatial and temporal scales: vegetation, atmosphere, climate and remote sensing. Landscape Ecology 2, 3–22.

Jensen, J.R., Cowen, D.J., Halls, J., Narumalani, S., Schmidt, N.J., Davis, B.A., Burgess, B., 1994. Improved urban infrastructure mapping and forecasting for Bellsouth using remote sensing and GIS technology. Photogrammetric Engineering and Remote Sensing 60, 339–346.

Leonardi, G., Papageorgiou, Y.Y., 1992. Conceptual foundation of spatial choice models. Environment and Planning A24, 1393–1408.

Li, H., Reynolds, J.F., 1997. Modeling effects of spatial pattern, drought, and grazing on rates of rangeland degradation: a combined Markov and cellular automaton approach. In: Quattrochi, D.A., Goodchild, M.F. (Eds.), Scale in Remote Sensing and GIS. Lewis Publishers, Boca Raton, Florida, pp. 211–230.

Liu, J., Ashton, P.S., 1998. FORMOSAIC: an individual-based spatially explicit model for simulating forest dynamics in landscape mosaics. Ecological Modelling 106, 177–200.

Lo, C.P., Faber, B.J., 1997. Integration of Landsat thematic mapper and census data for quality of life assessment. Remote Sensing of Environment 62, 143–157.

Mansfield, E., 1982. Micro-Economics: Theory & Applications. W.W. Norton and Company, Inc., New York, pp. 57–63.

Muller, M.R., Middleton, J., 1994. A Markov model of land-use change dynamics in the Niagara Region, Ontario, Canada. Landscape Ecology 9, 151–157.

NIPC, 1998. Population, household and employment forecasts for northeastern Illinois 1990 to 2020. Northeastern Illinois Planning Commission, Chicago, pp. 1–25.

O'Neill, R.V., Krummel, J.R., Gardner, R.H., Sugihari, G., Jackson, B., DeAngelis, D.L., Milne, B.T., Turner, M.G., Zygmunt, G., Christensen, S.W., Dale, V.H., Graham, R.L., 1988. Indices of landscape pattern. Landscape Ecology 3, 153–162.

O'Neill, R.V., Johnson, A.R., King, A.W., 1989. A hierarchical framework for the analysis of scale. Landscape Ecology 3, 193–205.

Openlands Project, 1999. Under Pressure: Land Consumption in the Chicago Region 1998–2028. Openlands Project, Chicago, pp. 1–31.

Parrot, R., Stutz, F.P., 1991. Urban GIS application. In: Maguire, D.J., Goodchild, M.F., Rhind, D.W. (Eds.), Geographical Information Systems: Principles And Application. Longman, London, pp. 247–260.

Peterson, W., 1989. Principles of Economics: Micro. Richard D. Irwin, Inc, Homewood, Illinois, pp. 37–43.

Sher, W., Pinola, R., 1981. Microeconomic Theory: A Synthesis of Classical Theory and the Modern Approach. Elsevier North Holland, Inc, New York, pp. 185–191.

Silvertown, J., Holtier, S., Johnson, J., Dale, P., 1992. Cellular automaton models of interspecific competition for space-the effect of pattern on process. Journal of Ecology 80, 527–534.

Timmerman, H., Borgers, A., 1989. Dynamic models of choice behavior: some fundamentals and trends. In: Hauer, J. (Ed.), Urban Dynamics and Spatial Choice Behavior. Kluwer Academic Publishers, pp. 3–26.

Turner, M.G., 1987. Spatial simulation of landscape changes in Georgia: a comparison of three transition models. Landscape Ecology 1, 29–36.

Turner, M.G., Costanza, R., Sklar, F.H., 1989. Methods to evaluate the performance of spatial simulation models. Ecological Modelling 48, 1–18.

Wu, F., 1998. SimLand: a prototype to simulate land conversion through the integrated GIS and CA with AHP-derived transition rules. International Journal of Geographical Information Sciences 12, 63–82.

Xie, Y., 1996. A generalized model for cellular urban dynamics. Geographical Analysis 28, 350–373.

Zhang, X., He, J., 1997. Urban spatial growth and spatio-temporal pattern of urban land development. Journal of Remote Sensing 1, 145–151 in Chinese with English abstract.

Zhou, G., Liebhold, A.M., 1995. Forecasting the spread of gypsy moth outbreaks using cellular transition models. Landscape Ecology 10, 177–186.